Neutrosophic Laplace Distribution with Properties and Applications in Decision Making

Ahmedia Musa M. Ibrahim*[1], Zahid Khan[2]

[1] Department of Business Administration, College of Sciences and the Human Sciences in Al Aflaj, Prince Sattam Bin Abdulaziz University, Al-Kharj, Saudi Arabia
[2] Department of Quantitative Methods, Pannon Egyetem, Veszprem, H-8200, Hungary.
Emails: am.ibrahim@psau.edu.sa; khan.zahid@gtk.uni-pannon.hu

Abstract

This paper introduces the concept of the neutrosophic Laplace distribution (LD_N), a probability distribution derived from the Laplace distribution. The LD_N offers a versatile framework for describing various real-world problems. We highlight the neutrosophic extension of the Laplace distribution and explore its applications in different areas. Extensive investigations into the mathematical properties of the distribution are presented, including the derivation of its probability density function, mean, variance, raw moment, skewness, and kurtosis. To estimate the parameters of the LD_N, we employ the method of maximum likelihood (ML) estimation within a neutrosophic environment. Furthermore, we conduct a simulation study to assess the effectiveness of the maximum likelihood approach in estimating the parameters of this new distribution. The findings demonstrate the potential of the LD_N in modeling and analyzing real-world phenomena. Eventually, some illustrative examples related to system reliability are provided to clarify further the implementation of the neutrosophic probabilistic model in real-world problems.

Keywords: Neutrosophic probability; Laplace distribution; maximum likelihood estimation; simulation

1. Introduction

The Laplace distribution is a probability distribution that can be derived from the exponential distribution and is commonly used for analyzing and modeling real-world problems. It is also known as the "law of the difference between two exponential distributed random variables," which highlights its connection to exponential distributions. This distribution is sometimes referred to as the "two-tailed distribution" or the "double exponential distribution." While its tails decay faster than those of the Cauchy distribution, they are less sharp compared to the Gaussian distribution [1].

The renowned economist J.M. Keynes [2] discussed the Laplace distribution in one of the earliest English language sources, describing it as a law of error. This distribution [3] finds applications in various fields such as economics, life sciences, and stochastic modeling. It plays a similar role under geometric summation as the Gaussian distribution does under ordinary summation. Additionally, the Laplace distribution characterizes errors in timing devices subjected to periodic excitation, as demonstrated by McGill in 1962 [4].

While the normal distribution [5] has commonly been used as an alternative to the Laplace distribution, the Laplace distribution has gained significant interest due to its intriguing applications in modeling. One of its key features is its ability to represent the likelihood of deviations or mistakes from a central value. In the field of astronomy, several astronomers are currently working on determining the distance of celestial objects from different points on Earth [6]. Hsu [7] discusses instances in sea and air navigation where accurately predicting the distribution of position mistakes in vessels and aircraft, obtained by combining data from complex navigation systems, is crucial.

Doi: https://doi.org/10.54216/IJNS.230106
Received: October 05, 2023 Revised: November 01, 2023 Accepted: November 12, 2023

Simon [8] is credited with discovering this distribution in 1774. In recent years, the Laplace distribution and similar distributions have garnered attention due to their resilience qualities, making them appealing for various applied research fields [9].

This work introduces the notion of the LD_N with the main goal of integrating unclear knowledge about the research variables. The best of our knowledge, no research has previously examined the neutrosophic structure of the laplace districution. The key mathematical properties of the suggested neutrosophic laplace distribution have been discussed in this study. Uncertain study parameters must be included in the model that represents a data-generating process since they cannot be ignored for practical analysis. This study proposes a unique extension to increase the application of the Laplace distribution in applied statistical research. Specifically, when fitting pollutant concentration data, the LD_N group is incorporated, which consists of several elements exhibiting a highly reasonably frequent distribution.

The motivation for this generalization stems from Smarandache's exploration of neutrosophy, a concept that deals with claims that are false, true, inconsistent, neutral, uncertain, or somewhere in between [10]. Neutrosophy logic [11]-[13] helps in studying data that exhibit indeterminacy in various real-world scenarios [14]-[17]. Neutrosophic statistics is employed to handle such data, as it extends classical statistics to address incomplete, ambiguous, confusing, or uncertain measurements [18]-[20]. Recently, the utilization of neutrosophic statistics has gained significant attention due to its favorable qualities, particularly when traditional statistics fail to accommodate the types of data [21]-[23]. Applied research has also employed neutrosophic statistics, as seen in literature references [24]-[26]. Furthermore, neutrosophic statistics has contributed to the study of indeterminacy effects in statistical process control [25]-[31].

The study remaining sections are organized as follows: The introduction of LD_N provides in Section 2. The mathematical strategy used to identify unidentified distributional variables is described in Section 3. In Section 4, a Monte Carlo simulation is performed to verify the theoretical outcomes of the neutrosophic model. An application of the suggested model is described in Section 5. The major study findings are finally presented in Section 6.

2. Proposed Model

A continuous random variable $\mathcal{Z}$ is said to follow neutrosophic Laplace distribution (LD_N) with two parameters if its pdf is of the form:

$$g_N(z) = \frac{1}{2\lambda_N} \exp\left(-\frac{|\mathcal{Z}-\mu_N|}{\lambda_N}\right), -\infty < Z < \infty, \ -\infty < \mu_N < \infty, \ \lambda_N \geq 0 \quad (1)$$

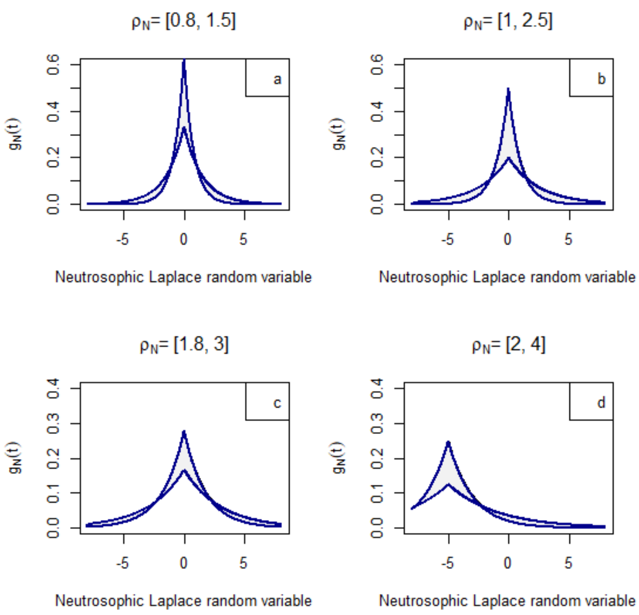

Figure 1: PDF plots of the proposed model

Doi: https://doi.org/10.54216/IJNS.230106
Received: October 05, 2023 Revised: November 01, 2023 Accepted: November 12, 2023

where $\mu_N = [\mu_l, \mu_u]$ is the neutrosophic location and $\lambda_N = [\lambda_l, \lambda_u]$ is the neutrosophic scale parameters respectively of the LD_N . Note that when $\mu_l = \mu_u = \mu$ and $\lambda_l = \lambda_u = \lambda LD_N$ convert to the current Laplace distribution.

Another key function of the LD_N is the cumulative function (CDF). This CDF is used to estimate the likelihood that a certain number of operational objects will fail in less than or equal to the specified period. If it's CDF is the form of:

$$g_N(\mathcal{Z}) = \frac{1}{2}\exp\left(\frac{\mathcal{Z}-\mu_N}{\lambda_N}\right), \text{if } \mathcal{Z} \le \mu_N \tag{2}$$

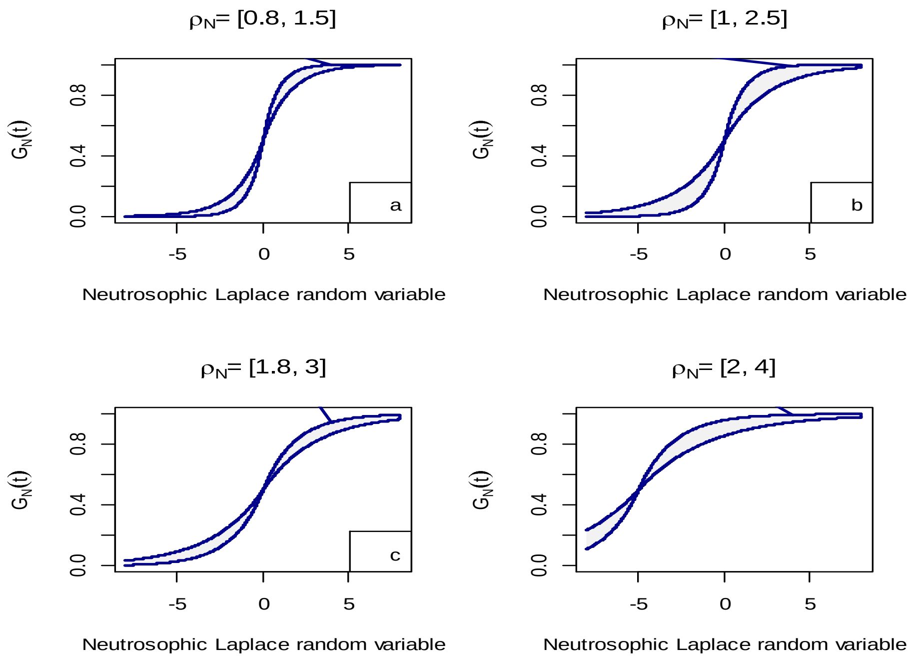

Figure 2: CDF plots of the proposed model

Definition 1: If $\mathcal{Z}$ follows the LD_N then $E(\mathcal{Z}) = \mu_N$

Proof: By definition the mean of the LD_N is:

$$E(\mathcal{Z}) = \int_{-\infty}^{\infty} \mathcal{Z}\frac{1}{2\lambda_N}\exp\left(-\frac{|\mathcal{Z}-\mu_N|}{\lambda_N}\right)d\mathcal{Z} \tag{3}$$

$$= \frac{1}{2\lambda_N}\int_{-\infty}^{\mu_N} \mathcal{Z}\exp\left(\frac{\mathcal{Z}-\mu_N}{\lambda_N}\right)d\mathcal{Z} + \frac{1}{2\lambda_N}\int_{\mu_N}^{\infty} \mathcal{Z}\exp\left(\frac{-\mathcal{Z}+\mu_N}{\lambda_N}\right)d\mathcal{Z}$$

$$= \left[\frac{1}{2\lambda_l}\int_{-\infty}^{\mu_l} \mathcal{Z}\exp\left(\frac{\mathcal{Z}-\mu_l}{\lambda_l}\right)d\mathcal{Z}, \frac{1}{2\lambda_u}\int_{-\infty}^{\mu_u} \mathcal{Z}\exp\left(\frac{\mathcal{Z}-\mu_u}{\lambda_u}\right)d\mathcal{Z}\right] + \left[\frac{1}{2\lambda_l}\int_{\mu_l}^{\infty} \mathcal{Z}\exp\left(\frac{-\mathcal{Z}+\mu_l}{\lambda_l}\right)d\mathcal{Z}, \frac{1}{2\lambda_u}\int_{\mu_u}^{\infty} \mathcal{Z}\exp\left(\frac{-\mathcal{Z}+\mu_u}{\lambda_u}\right)d\mathcal{Z}\right] \tag{4}$$

Equ (4) integration by parts

$$\left[\frac{1}{2\lambda_l}\int_{-\infty}^{\mu_l} \mathcal{Z}\exp\left(\frac{\mathcal{Z}-\mu_l}{\lambda_l}\right)d\mathcal{Z} + \frac{1}{2\lambda_l}\int_{\mu_l}^{\infty} \mathcal{Z}\exp\left(\frac{-\mathcal{Z}+\mu_l}{\lambda_l}\right)d\mathcal{Z}\right] = \mu_l$$

And

$$\left[\frac{1}{2\lambda_u}\int_{-\infty}^{\mu_u} \mathcal{Z}\exp\left(\frac{\mathcal{Z}-\mu_u}{\lambda_u}\right)d\mathcal{Z} + \frac{1}{2\lambda_u}\int_{\mu_u}^{\infty} \mathcal{Z}\exp\left(\frac{-\mathcal{Z}+\mu_u}{\lambda_u}\right)d\mathcal{Z}\right] = \mu_u$$

So,

Doi: https://doi.org/10.54216/IJNS.230106
Received: October 05, 2023 Revised: November 01, 2023 Accepted: November 12, 2023

$\mu_N = [\mu_l, \mu_u]$, hence proved.

Definition 2: If $\mathcal{Z}$ follows the LD_N, The variance of $\mathcal{V}_N(\mathcal{Z}) = 2\lambda_N^2$

Proof: Noting that variance of the LD_N is:

$$\mathcal{V}_N(\mathcal{Z}) = E(\mathcal{Z}^2) - [E(\mathcal{Z})]^2 \tag{5}$$

And

$$E(\mathcal{Z}^2) = \int_{-\infty}^{\infty} \mathcal{Z}^2 \frac{1}{2\lambda_N} \exp\left(-\frac{|\mathcal{Z}-\mu_N|}{\lambda_N}\right) d\mathcal{Z} \tag{6}$$

$$= \frac{1}{2\lambda_N}\int_{-\infty}^{\mu_N} \mathcal{Z}^2 \exp\left(\frac{\mathcal{Z}-\mu_N}{\lambda_N}\right) d\mathcal{Z} + \frac{1}{2\lambda_N}\int_{\mu_N}^{\infty} \mathcal{Z}^2 \exp\left(\frac{-\mathcal{Z}+\mu_N}{\lambda_N}\right) d\mathcal{Z}$$

$$= \left[\frac{1}{2\lambda_l}\int_{-\infty}^{\mu_l} \mathcal{Z}^2 \exp\left(\frac{\mathcal{Z}-\mu_l}{\lambda_l}\right) d\mathcal{Z}, \frac{1}{2\lambda_u}\int_{-\infty}^{\mu_u} \mathcal{Z}^2 \exp\left(\frac{\mathcal{Z}-\mu_u}{\lambda_u}\right) d\mathcal{Z}\right] + \left[\frac{1}{2\lambda_l}\int_{\mu_l}^{\infty} \mathcal{Z}^2 \exp\left(\frac{-\mathcal{Z}+\mu_l}{\lambda_l}\right) d\mathcal{Z}, \frac{1}{2\lambda_u}\int_{\mu_u}^{\infty} \mathcal{Z}^2 \exp\left(\frac{-\mathcal{Z}+\mu_u}{\lambda_u}\right) d\mathcal{Z}\right]$$

Further simplification provides;

$$\left[\frac{1}{2\lambda_l}\int_{-\infty}^{\mu_l} \mathcal{Z}^2 \exp\left(\frac{\mathcal{Z}-\mu_l}{\lambda_l}\right) d\mathcal{Z} + \frac{1}{2\lambda_l}\int_{\mu_l}^{\infty} \mathcal{Z}^2 \exp\left(\frac{-\mathcal{Z}+\mu_l}{\lambda_l}\right) d\mathcal{Z}\right] = \mu_l^2 + 2\lambda_l^2$$

And

$$\left[\frac{1}{2\lambda_u}\int_{-\infty}^{\mu_u} \mathcal{Z}^2 \exp\left(\frac{\mathcal{Z}-\mu_u}{\lambda_u}\right) d\mathcal{Z} + \frac{1}{2\lambda_u}\int_{\mu_u}^{\infty} \mathcal{Z}^2 \exp\left(\frac{-\mathcal{Z}+\mu_u}{\lambda_u}\right) d\mathcal{Z}\right] = \mu_u^2 + 2\lambda_u^2$$

Thus becomes equ (6)

$\mathcal{V}_N(\mathcal{Z}) = [2\lambda_l^2, 2\lambda_u^2] = 2\lambda_N^2$, hence proved.

Definition 3: Show that k^{th} raw moment of the LDN is μ_N^k

Proof: Noting that the k^{th} moment of the LD_N is:

$$\mu_{kN}''(\mathcal{Z}) = \int_{-\infty}^{\infty} \mathcal{Z}^k \frac{1}{2\lambda_N} \exp\left(-\frac{|\mathcal{Z}-\mu_N|}{\lambda_N}\right) d\mathcal{Z} \tag{7}$$

$$= \frac{1}{2\lambda_N}\int_{-\infty}^{\mu_N} \mathcal{Z}^k \exp\left(\frac{\mathcal{Z}-\mu_N}{\lambda_N}\right) d\mathcal{Z} + \frac{1}{2\lambda_N}\int_{\mu_N}^{\infty} \mathcal{Z}^k \exp\left(\frac{-\mathcal{Z}+\mu_N}{\lambda_N}\right) d\mathcal{Z}$$

$$= \left[\frac{1}{2\lambda_l}\int_{-\infty}^{\mu_l} \mathcal{Z}^k \exp\left(\frac{\mathcal{Z}-\mu_l}{\lambda_l}\right) d\mathcal{Z}, \frac{1}{2\lambda_u}\int_{-\infty}^{\mu_u} \mathcal{Z}^k \exp\left(\frac{\mathcal{Z}-\mu_u}{\lambda_u}\right) d\mathcal{Z}\right] + \left[\frac{1}{2\lambda_l}\int_{\mu_l}^{\infty} \mathcal{Z}^k \exp\left(\frac{-\mathcal{Z}+\mu_l}{\lambda_l}\right) d\mathcal{Z}, \frac{1}{2\lambda_u}\int_{\mu_u}^{\infty} \mathcal{Z}^k \exp\left(\frac{-\mathcal{Z}+\mu_u}{\lambda_u}\right) d\mathcal{Z}\right] \tag{8}$$

Equ (8) integration by parts

$$\left[\frac{1}{2\lambda_l}\int_{-\infty}^{\mu_l} \mathcal{Z}^k \exp\left(\frac{\mathcal{Z}-\mu_l}{\lambda_l}\right) d\mathcal{Z} + \frac{1}{2\lambda_l}\int_{\mu_l}^{\infty} \mathcal{Z}^k \exp\left(\frac{-\mathcal{Z}+\mu_l}{\lambda_l}\right) d\mathcal{Z}\right] = \mu_l^k$$

And

$$\left[\frac{1}{2\lambda_u}\int_{-\infty}^{\mu_u} \mathcal{Z}^k \exp\left(\frac{\mathcal{Z}-\mu_u}{\lambda_u}\right) d\mathcal{Z} + \frac{1}{2\lambda_u}\int_{\mu_u}^{\infty} \mathcal{Z}^k \exp\left(\frac{-\mathcal{Z}+\mu_u}{\lambda_u}\right) d\mathcal{Z}\right] = \mu_u^k$$

So,

$\mu_N^k = [\mu_l^k, \mu_u^k]$, where $k = 1,2, \ldots$, the k^{th} moment about the origin of the LDN distribution.

Doi: https://doi.org/10.54216/IJNS.230106
Received: October 05, 2023 Revised: November 01, 2023 Accepted: November 12, 2023

$$\mu'_{1N} = \mu''_{1N} = \mu_N$$

$$\mu'_{2N} = \mu''_{2n} - (\mu''_{1n})^2 = \mu_N^2 + 2\lambda_N^2$$

$$\mu'_{3N} = \mu''_{3n} - 3\mu''_{2n}\mu''_{1n} + 2(\mu''_{1n})^3 = \mu_N^3 + 6\mu_N\lambda_N^2$$

$$\mu'_{4N} = \mu''_{4n} - 4\mu''_{3n}\mu''_{1n} - 3(\mu''_{2n})^2 + 12\mu''_{2n}(\mu''_{1n})^2 - 6(\mu''_{1n})^4 = \mu_N^4 + 12\mu_N^2\lambda_N^2 + 24\lambda_N^4$$

Definition 4: Show that the coefficient of skewness for the LD_N is 0.

Proof: The coefficient of skewness for LD_N is given by:

$$\eta'_{1N} = \frac{\mu'_{3N}}{(\mu'_{2N})^{3/2}} \tag{9}$$

Where

$\mu'_{2N} = \mu_N^2 + 2\lambda_N^2$ and $\mu'_{3N} = \mu_N^3 + 6\mu_N\lambda_N^2$

By substituting (9) provides;

$$\eta'_{1N} = \frac{\mu_N^3 + 6\mu_N\lambda_N^2}{(\mu_N^2 + 2\lambda_N^2)^{3/2}}$$

$\eta'_{1N} = [0,0]$, hence proved.

Definition 5: Show that the coefficient of kurtosis for LD_N is 6.

Proof: By definition the coefficient of kurtosis is given by:

$$\eta_{2N} = \frac{\mu'_{4N}}{{\mu'_{2N}}^2} \tag{10}$$

Where $\mu'_{4N} = \mu_N^4 + 12\mu_N^2\lambda_N^2 + 24\lambda_N^4$ and $\mu'_{2N} = \mu_N^2 + 2\lambda_N^2$

By substituting (9) provides;

$$\eta'_{2N} = \frac{\mu_N^4 + 12\mu_N^2\lambda_N^2 + 24\lambda_N^2}{(\mu_N^2 + 2\lambda_N^2)^2}$$

where

$\eta'_{2N} = [6,6]$, hence proved.

Note that the mean, variance are indeterminate values whereas sknewness and kurtosis are crisps values. For different values fixed value of $\mu_N = [0, 0]$ and different values of λ_N are calculated and shown in Table 1

Table 1: Descriptive statistics based on analytical results of the proposed model

λ_N	Mean	Variance	Mode	Skewness	Kurtosis
[0.5, 1]	[0, 0]	[0.5, 2]	[0, 0]	[0, 0]	[6, 6]
[1.5, 2]	[0, 0]	[4.5, 8]	[0,0]	[0, 0]	[6, 6]
[3,4]	[0, 0]	[18, 32]	[0,0]	[0, 0]	[6, 6]
[4,5]	[0, 0]	[32, 50]	[0,0]	[0, 0]	[6, 6]

Table 1 reveals an intriguing finding: when the scale parameter varied, it introduced a certain level of uncertainty in estimating the variance of the suggested model. Nevertheless, it is important to point out that intervals with equal lower and upper bounds consistently produced accurate and clear values, aligning with what was expected from the model.

This result emphasizes how changes in the scale parameter affect variance and underscores the dependability of the model within particular parameter intervals.

Doi: https://doi.org/10.54216/IJNS.230106
Received: October 05, 2023 Revised: November 01, 2023 Accepted: November 12, 2023

There are some important functions in context of Laplace distribution that commonly used in reliability theory. In probability and statistics, the survival function is fundamental to the study and practice of modelling data with survival or lifespan features. The survival function plays a crucial role in elucidating the characteristics and practical utility of the Laplace distribution. The survival function of the proposed model can be defined as:

$$S_N(z) = P[Z > z] = \int_z^{\infty} \frac{1}{2\lambda_N} \exp\left(-\frac{|\mathcal{Z} - \mu_N|}{\lambda_N}\right) dz$$

Simplifying the integral provides:

$$S_N(z) = \exp\left(-\frac{|\mathcal{Z} - \mu_N|}{\lambda_N}\right) \tag{11}$$

The graph of $S_N(z)$ function for different values of different values of neutrosophic parameters are shown in Figure 3

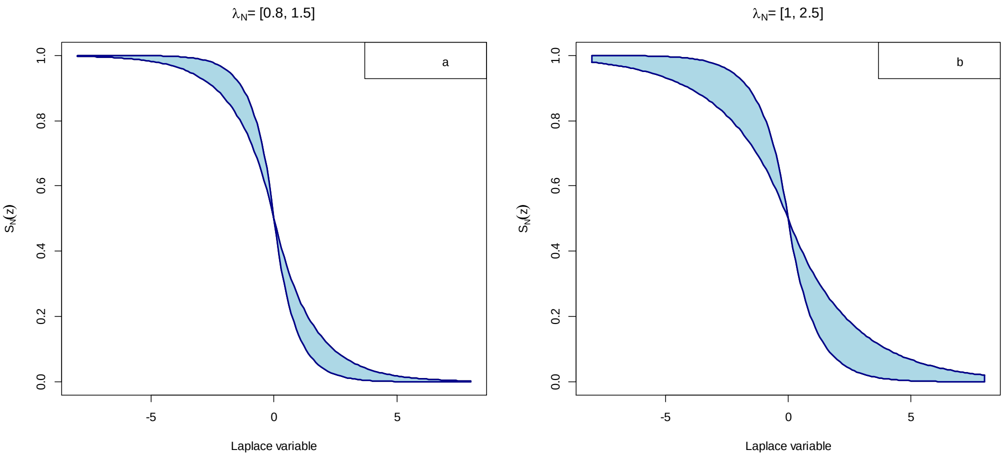

Figure 3: Survival curve of the proposed model

Figure 3 shows that the suggested model exhibits a clear exponential decay pattern in its survival curve, making it highly suitable for modeling data with survival or lifetime characteristics. This implies that as time or the event being studied progresses, the likelihood of the event not happening decreases exponentially. Additionally, an essential aspect of reliability theory is the hazard function, which can be defined for this proposed model as follows:

$$H_N(z) = \frac{g_N(z)}{S_N(z)} = \frac{1}{2\lambda_N} \tag{12}$$

The hazard curve of the proposed model is depicted in Figure 4.

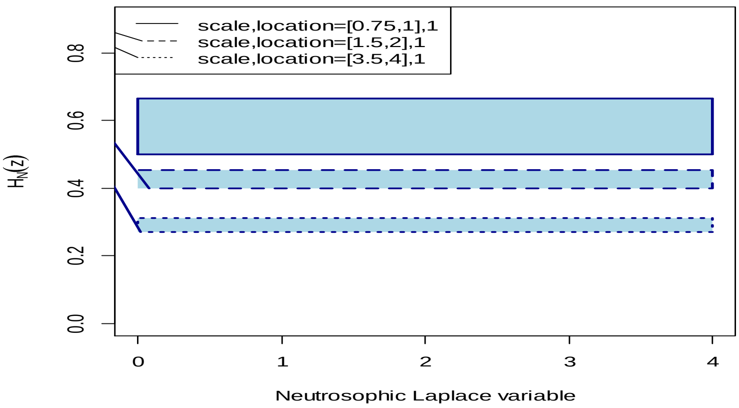

Figure 4: Hazard function of the proposed model

Doi: https://doi.org/10.54216/IJNS.230106
Received: October 05, 2023 Revised: November 01, 2023 Accepted: November 12, 2023

The hazard function of the suggested model is a constant, indicating that the hazard does not change with z. This means that the hazard rate remains the same regardless of the value of time or the point on the x-axis. The constant hazard rate $\frac{1}{2\lambda_N}$ dicates that the risk of the event occurring is uniform and does not change over time. This property is unique to the Laplace distribution and stands in contrast to many other survival distributions where the hazard rate changes over time. Thus, the hazard function of the Laplace distribution is distinguished by a steady, flat line that indicates a consistent and uniform hazard rate. This specific characteristic is exclusive to the Laplace distribution and carries significance in comprehending the distribution's features, its relevance in survival analysis, and its resilience against outliers and extreme values.

3. Estimation Procedure

The estimation procedure of the LD_N involves using maximum likelihood estimation (MLE) to estimate the parameters. MLE aims to find the parameter values that maximize the likelihood of observing the given data. In the case of the Laplace distribution, the parameters to be estimated are the location parameter (μ_N) and scale parameter (λ_N). By maximizing the likelihood function, we can obtain estimates for μ_N and $\lambda_N$that best fit the observed data.

Let a dataset $Z = \{z_1, z_2, \dots z_n\}$ assumed to be independently and identically distributed according to the proposed neutrosophic model with parameters μ_N and λ_N.

The likelihood function for the LD_N is

$$\xi(\mu_N, \lambda_N \mid Z) = \prod_{i=1}^{n} \frac{1}{2\lambda_N} \exp\left(-\frac{|z_i - \mu_N|}{\lambda_N}\right) \quad (13)$$

By simplifying calculations, the natural logarithm of the (13) can be taken without altering the position of the maximum.

$$\ln \xi(\mu_N, \lambda_N \mid Z) = -n \ln(2\lambda_N) - \frac{1}{\lambda_N} \sum_{i=1}^{n} |z_i - \mu_N| \quad (14)$$

To maximize with respect to μ_N, we differentiate the (14) with respect to μ_N and set the derivative equal to zero.

$$\frac{\delta \ln \xi(\mu_N, \lambda_N \mid Z)}{\delta \mu_N} = \frac{1}{\lambda_N} \sum_{i=1}^{n} \operatorname{sign}(z_i - \mu_N) = 0 \quad (15)$$

Solving (15) for μ_N leads to:

$$\sum_{i=1}^{n} \operatorname{sign}(z_i - \mu_N) = 0 \quad (16)$$

Equation (16) states that the sum of the signs of the deviations of the data points from μ_N is zero. This leads to the MLE of μ_N, which is the median of the data.

To maximize with respect to λ_N, we differentiate the log-likelihood function with respect to λ_N and set the derivative equal to zero.

This yields:

$$\lambda_N = \frac{1}{n} \sum_{i=1}^{n} |z_i - \mu_N| \quad (17)$$

Thus expressions (16) and (17) provide neutrosophic estimates for the location and scale parameters that maximize the likelihood of the observed data under the proposed LD_N.

4. Simulation Assessment

In this section, we have explored the theoretical foundations and examined some important distributional characteristics of the proposed NLD in the neutrosophic framework. For simplicity, the distribution characteristics that are parameterized as shown in (6) and (7) are provided below:

The quantile function of the LD_N, also known as the inverse CDF, is a mathematical function that calculates the value at which a given probability is reached. It is commonly used in statistical analysis and modeling to determine percentiles and critical values associated with the Laplace distribution. The following assertion is the basis of the inverse transformation approach, which acts as a general method for simulating a random sample from the neutrosophic model.

Doi: https://doi.org/10.54216/IJNS.230106
Received: October 05, 2023 Revised: November 01, 2023 Accepted: November 12, 2023

The quantile function (inverse cumulative distribution function) of the LD_N with location parameter μ_N and scale parameter λ_N is given by:

$$\varrho(t, \mu_N, \lambda_N) = \mu_N - \lambda_N \text{sign}(t - 0.5)\ln(1 - 2|t - 0.5|) \quad (18)$$

Here, $\varrho(t, \mu_N, \lambda_N)$ represents the quantile value corresponding to the cumulative probability t, μ is the location parameter, μ_N is the scale parameter λ_N, and $\text{sign}(t)$ returns +1 for positive values of t and -1 for negative values of$t$. The cumulative probability t is in the range zero and 1. This formula maps a given cumulative probability t to the corresponding quantile value from the Laplace distribution with the specified parameters. The quantile function is commonly used in statistics to determine the value at which a given probability occurs in a distribution. It allows for the calculation of specific percentiles or quantiles, such as the median or quartiles, based on the location and scale parameters of the distribution. This function can be harnessed to generate random data that accurately reflects the density outlined in equation (1). The analytical outcomes encompassing mean, variance, and estimated values of parameters can undergo validation through Monte Carlo simulation.

To validate theory-derived conclusions, a practical approach is to follow a straightforward process. This involves selecting specific values for the parameters λ_N ranging from 1.5 to 3 and μ_N ranging from 0.5 to 1. By setting these parameters, a dataset of 10,000 random samples is generated from a uniform distribution. These random samples are then transformed into 10,000 pseudo neutrosophic random samples using equation (18), effectively representing the LD_N. We utilize simulated datasets which serve as empirical evidence to support the analytical properties discussed in Section 2 of our study. We conduct a thorough examination and comparison of various statistical characteristics such as mean, variance, and estimated parametric values of the proposed model. The results of this analysis are presented in Table 2, enabling us to evaluate the agreement between the theoretical and simulated outcomes.

Table 2: Estimated values of the proposed model based on simulated data

Sample Size	Estimated μ_N	Estimated λ_N	Estimated Mean	Estimated Standard Deviation
20	[1.08, 1.78]	[1.15, 1.31]	[1.08, 1.78]	[1.63, 1.85]
50	[0.72, 1.41]	[0.99, 1.99]	[0.72, 1.41]	[1.40, 2.82]
80	[0.46, 0.92]	[1.00, 2.00]	[0.46, 0.92]	[1.42, 2.84]
100	[0.58, 1.17]	[0.77, 1.54]	[0.58, 1.17]	[1.09, 2.18]
150	[0.46, 0.93]	[0.90, 1.80]	[0.46, 0.93]	[1.27, 2.54]

Table 2 presents the estimated values of specific statistical properties of the proposed model, which have been calculated for various sample sizes. In order to simplify the computation process, the sample sizes have been set at fixed precise values, although they can also be imprecise. These estimated values have been obtained by utilizing ML estimation as defined in Section 3. As the number of observations in the sample increases, the estimates for μ_N and λ_N become more accurate and less subject to variation. For instance, when comparing a sample size of 20 to 150, the range of estimated values becomes narrower. This indicates that larger sample sizes allow for more precise estimates of the parameters. As the sample size increases, both the estimated mean and standard deviation values show a similar pattern. The range of estimated values becomes narrower, signifying enhanced precision with larger samples. It is encouraging to see that the estimated parameter values, mean, and standard deviation are within the specified ranges. This indicates that the simulations are in line with theoretical expectations, which further supports the validity of the proposed model.

5. Application to Real World Data

In this section, we will examine a genuine dataset that focuses on water levels in Bedfordshire, England. More specifically, we will analyze data from the Bedford Road Sluice Northampton Automation Monitoring Station. This dataset consists of daily measurements gathered by the Environment Agency's network of monitoring stations [32]. Valuable information can be accessed from this separate website where data from different sources is combined. This website offers a map that displays river levels and flood warnings in one place. Additionally, it provides in-depth information about each river level monitoring station in England and the corresponding flood warning areas. To carry out our analysis, we will be using data obtained from this platform. The data will cover daily observations specific time period from June 5, 2017, to July 2, 2017. Our goal is to apply the proposed

Doi: https://doi.org/10.54216/IJNS.230106
Received: October 05, 2023 Revised: November 01, 2023 Accepted: November 12, 2023

neutrosophic model to real-world water level observations in order to gain insights and make descriptive analysis. This analysis will help us better understand water level dynamics and assess potential flood risks in the Bedfordshire region.

Measuring the water level of a river can be quite challenging because it constantly fluctuates and is always changing. To overcome this challenge, we record both the lowest and highest water levels during a specific time period. These important measurements are then summarized in Table 3, giving us an idea of the variability that exists in the water levels of rivers in this particular region.

Table 3: Real data on water level collected at Bedford Road Sluice Northampton Automation Monitoring Station

Water level				
[55.94, 55.98]	[55.92, 55.96]	[55.93, 55.97]	[55.91, 55.98]	[55.88, 55.91]
[55.92, 55.95]	[55.93, 55.95]	[56.04, 56.05]	[56.00, 56.04]	[55.96, 55.99]
[55.95, 55.96]	[55.96, 55.98]	[55.96, 55.98]	[55.97, 55.98]	[55.95,55.98]
[55.95, 55.99]	[55.99, 56.02]	[56.01, 56.05]	[56.00, 56.02]	

To ensure the integrity of our analysis, it is crucial to first comprehend the distribution of the data before delving into our analytical journey and implementing our proposed model. In order to achieve this, we have created basic probability plots in Figure 5 that illustrate the average water levels over time. These records of average water levels can be easily obtained from the same reliable data source.

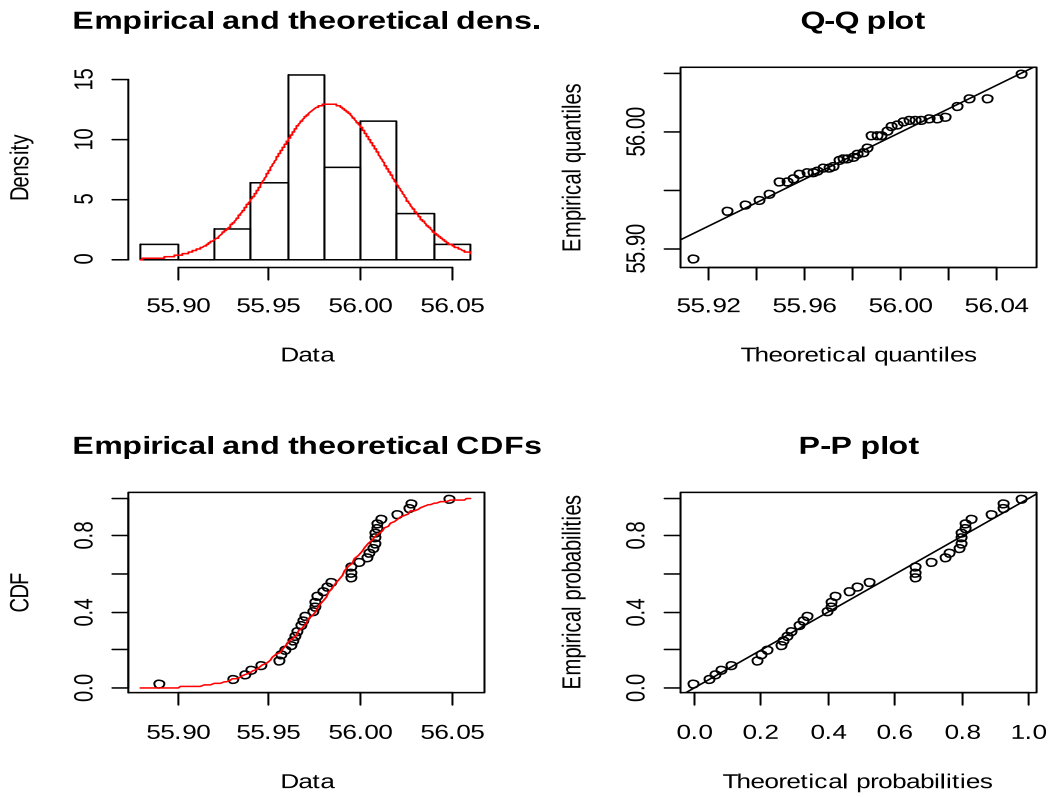

Figure 5: Basic fitting plots of the flood data

The results of our probability plots, as shown in Figure 5, provide interesting insights. The data demonstrates a balanced pattern, with observations evenly distributed above and below the central tendency. This symmetrical distribution implies that the Laplace distribution, which is renowned for its symmetric properties, could be a

Doi: https://doi.org/10.54216/IJNS.230106
Received: October 05, 2023 Revised: November 01, 2023 Accepted: November 12, 2023

suitable model for the observed data. The Laplace distribution, also known as the double-exponential distribution, is ideal for situations where data shows symmetry and resilience to outliers. Given the symmetrical nature of the average water level data, we can confidently consider the Laplace model as a suitable choice for further analysis.

The current form of our dataset presents a challenge for the conventional Laplace model. This is because the recorded water level values exhibit fluctuations and variability that do not align with the assumptions of a standard Laplace distribution. The imprecision in these values makes the Laplace model less suitable for analysing our dataset, which requires a different approach. To address this challenge, we have presented a proposed model that is tailor-made to handle the intricacies and inaccuracies found in our dataset. This groundbreaking model provides a versatile framework for efficiently capturing and analysing the water level data.

Table 4: Descriptive analysis of the real data using proposed model

Descriptive measures	Estimated values
Location Parameter	[55.95, 55.96]
Scale Parameter	[291.02, 291.03]
Mean	[55.95, 55.96]
Standard Deviation	[411.46, 511,53]
Mode	[55.95, 55.96]
Skewness	[0, 0]

Table 4 displays the outcomes of implementing the suggested model, which demonstrates its ability to effectively adjust to the distinct features of the water level measurements. Through utilizing this enhanced methodology, our objective is to obtain more precise and meaningful insights from the collected data. Table 4 displays the outcomes of implementing the suggested model, which demonstrates its ability to effectively adjust to the distinct features of the water level measurements. Through utilizing this enhanced methodology, our objective is to obtain more precise and meaningful insights from the collected data. The analysis presented in Table 4 emphasizes the importance of accounting for uncertainty in recorded observations. In conventional descriptive statistics, precise values are typically used to make conclusions about a dataset. However, for data like our water level measurements that inherently have imprecision and uncertainty, a different methodology is required. In Table 4, we observe a departure from the conventional, as our statistics take on an uncertain character. This shift acknowledges the reality that our data may not lend itself to the usual precision associated with statistical summaries. Instead, we embrace uncertainty as an integral part of our analysis, recognizing that it reflects the complex and dynamic nature of the recorded water level values. By including uncertainty in our descriptive statistics, we enhance the accuracy of our analysis and obtain a more realistic portrayal of the dataset. This methodology enables us to consider variations and uncertainties, leading to a more comprehensive comprehension of the patterns and trends within the water level data. By embracing this perspective, we can enhance our ability to tackle the difficulties brought about by uncertain data in the field of hydrology and flood management. Consequently, it empowers us to make more well-informed decisions.

6. Conclusions

In this work, we have introduced and explored the concept of the neutrosophic Laplace distribution (LD_N), a versatile probability distribution derived from the Laplace distribution. Our findings demonstrate that LD_N offers a reliable approach for addressing diverse real-world challenges. We have broadened the scope of the Laplace distribution by incorporating it into a neutrosophic context, allowing for its application in various fields. During our research, we thoroughly examined the mathematical characteristics of the LD_N, such as its probability density function and moments (mean, variance, skewness, and kurtosis). Additionally, we introduced the method of maximum likelihood (ML) estimation within the neutrosophic framework to accurately estimate the distribution's parameters. Furthermore, an evaluation of the ML approach in estimating parameters for this innovative distribution has been carried out through a simulation study. The outcomes obtained from our analysis have confirmed that LD_N has the capability to effectively model and analyze real-life phenomena. To demonstrate the practicality of our suggested approach, we have applied it to examine water levels in Bedfordshire, England. Specifically, we have utilized data from the Bedford Road Sluice Northampton Automation Monitoring Station. This case study showcases how LD_N can effectively handle fuzzy environmental data and emphasizes its potential for future use in different fields.

Doi: https://doi.org/10.54216/IJNS.230106
Received: October 05, 2023 Revised: November 01, 2023 Accepted: November 12, 2023

Acknowledgement: The authors extend their appreciation to Prince Sattam Bin Abdulaziz University for funding this research work through the project number (PSAU/2023/02/25019).

Conflicts of Interest: The authors declare no conflict of interest.

References

[1] Aryal, G. R., Study of Laplace and related probability distributions and their applications, Graduate School Theses and Dissertations, University of South Florida. 2006.

[2] Rosser Jr, J. B., Reconsidering periodicity and fundamental uncertainty, Journal of Post Keynesian Economics, 38(3), 331-354, 2015.

[3] George, D., & George, S., Marshall-Olkin Esscher transformed Laplace distribution and processes, Brazilian Journal of Probability and Statistics, 162-184, 2013.

[4] McGill, W. J., Random fluctuations of response rate, Psychometrika, 27(1), 3-17, 1962.

[5] Nekoukhou, V., & Alamatsaz, M. H., A family of skew-symmetric-Laplace distributions, Statistical papers, 53(3), 685-696, 2012.

[6] Geraci, M., & Borja, M. C., Notebook: The Laplace distribution, 2018.

[7] Hsu, D. A., Long-tailed distributions for position errors in navigation, Journal of the Royal Statistical Society: Series C (Applied Statistics), 28(1), 62-72, 1979.

[8] Wilson, E. B., First and second laws of error, Journal of the American Statistical Association, 18(143), 841-851, 1923.

[9] Kozubowski, T. J., & Nadarajah, S., Multitude of Laplace distributions, Statistical Papers, 51(1), 127, 2010.

[10] Smarandache, F., Neutrosophic logic: generalization of the Intuitionistic fuzzy logic, Extr. Metal. Nickel Cobalt Platin. Group Metals, 269(50), 49-53, 2016.

[11] Smarandache, F., A unifying field in logics: neutrosophic logic. Neutrosophy, neutrosophic set, neutrosophic probability: neutrsophic logic, 2005.

[12] Khalid, H. E., Smarandache, F., & Essa, A. K., The basic notions for (over, off, under) neutrosophic geometric programming problems, Infinite Study, 2018.

[13] Smarandache, F., Neutrosophy: neutrosophic probability, set, and logic: analytic synthesis & synthetic analysis, 1998.

[14] Smarandache, F., Introduction to Neutrosophic Statistics, Sitech & Education Publishing, Craiova, 2014, 124 p.

[15] Duan, W. Q., Khan, Z., Gulistan, M., & Khurshid, A., Neutrosophic exponential distribution: Modeling and applications for complex data analysis, Complexity, 2021, 1-8.

[16] Patro, S. K., & Smarandache, F., The neutrosophic statistical distribution, more problems, more solutions, Infinite Study, 2016.

[17] Aslam, M., A variable acceptance sampling plan under neutrosophic statistical interval method, Symmetry, 11(1), 114, 2019.

[18] Schweizer, P., Uncertainty: two probabilities for the three states of neutrosophy, International Journal of Neutrosophic Science, 2(1), 18-26, 2020.

[19] Arif, O. H., & Aslam, M., A new sudden death chart for the Weibull distribution under complexity, Complex & Intelligent Systems, 7, 2093-2101, 2021.

[20] Aslam, M., Analyzing wind power data using analysis of means under neutrosophic statistics, Soft Computing, 25(10), 7087-7093, 2021.

[21] Aslam, M., Arif, O. H., & Sherwani, R. A. K., New diagnosis test under the neutrosophic statistics: an

Doi: https://doi.org/10.54216/IJNS.230106
Received: October 05, 2023 Revised: November 01, 2023 Accepted: November 12, 2023

application to diabetic patients, BioMed Research International, 2020.

[22] Chen, J., Ye, J., Du, S., & Yong, R., Expressions of rock joint roughness coefficient using neutrosophic interval statistical numbers, Symmetry, 9(7), 123, 2017.

[23] Smarandache, F., & Savoiu, G., Neutrosophic index numbers: neutrosophic logic applied in the statistical indicators theory, A Publication of Society for Mathematics of Uncertainty, 10, 67, 2015.

[24] Aslam, M., Bantan, R. A., & Khan, N., Design of a new attribute control chart under neutrosophic statistics, International Journal of Fuzzy Systems, 21, 433-440, 2019.

[25] Khan, Z., Gulistan, M., Kadry, S., Chu, Y., & Lane-Krebs, K., On scale parameter monitoring of the Rayleigh distributed data using a new design, IEEE access, 8, 188390-188400, 2020.

[26] Khan, Z., Gulistan, M., Chammam, W., Kadry, S., & Nam, Y., A new dispersion control chart for handling the neutrosophic data, IEEE access, 8, 96006-96015, 2020.

[27] Khan, Z., Gulistan, M., Hashim, R., Yaqoob, N., & Chammam, W., Design of S-control chart for neutrosophic data: An application to manufacturing industry, Journal of Intelligent & Fuzzy Systems, 38(4), 4743-4751, 2020.

[28] Khan, Z., Gulistan, M., Kausar, N., & Park, C., Neutrosophic Rayleigh model with some basic characteristics and engineering applications, IEEE Access, 9, 71277-71283, 2021.

[29] M. Palanikumar,Aiyared Iampan,Said Broumi, MCGDM based on VIKOR and TOPSIS proposes neutrsophic Fermatean fuzzy soft with aggregation operators, International Journal of Neutrosophic Science, Vol. 19 , No. 3 , (2022) : 85-94 (Doi : https://doi.org/10.54216/IJNS.190308)

[30] P. Reena Joice,M. Trinita Pricilla,S. Broumi, Generalized Pre-closed Sets in Fermatean Neutrosophic Hypersoft Topological Spaces, International Journal of Neutrosophic Science, Vol. 20 , No. 3 , (2023) : 82-97 (Doi : https://doi.org/10.54216/IJNS.200308)

[31] Broumi, S., Sundareswaran, R., Shanmugapriya, M., Bakali, A., & Talea, M. Theory and Applications of Fermatean Neutrosophic Graphs. Neutrosophic Sets and Systems, 50, 248-286. 2022.

[32] Nabil M. AbdelAziz,Hassan H. Mohammed,Khalid A. Eldrandaly, An effective Decision making model through Fusion Optimization and risk associated with flash flood hazards: A case study Asyut, Egypt, Fusion: Practice and Applications, Vol. 12 , No. 1 , (2023) : 64-94 (Doi : https://doi.org/10.54216/FPA.120105)

Doi: https://doi.org/10.54216/IJNS.230106
Received: October 05, 2023 Revised: November 01, 2023 Accepted: November 12, 2023